Vol. 14(12), pp. 125-138, August, 2019
DOI: 10.5897/IJPS2019.4830
Article Number: 3158AED61658
ISSN: 1992-1950
Copyright ©2019
Author(s) retain the copyright of this article
http://www.academicjournals.org/IJPS

International Journal of Physical Sciences

Full Length Research Paper

Seasonal analyses of solar radiation on flat ground for different state of sky: Case of Nouakchott, Mauritania

Eslemhoum Jiddou ABDI[1]*, Mohamed Mahmoud ALI[1], Boudy BILAL[2], Nourou DIA[1], Mamoudou NDONGO[1], Ckeikh Mohamed Fadel KEBE[3] and Papa Alioune NDIAYE[3]

[1]Labotratoire de Recherche Appliquée aux Energies Renouvelables (LRAER)/FST/UNA, Mauritania.
[2]Département Mécanique, Ecole supérieure polytechnique (ESP), Mauritania.
[3]Centre International de Formation et de Recherche en Energie Solaire (C.I.F.R.E.S)/ESP/UCAD Sénégal.

Received 17 June, 2019; Accepted 6 August, 2019

This paper proposes a method to evaluate solar energy on flat ground for different state of sky (clear sky, moderately covered sky and covered sky). Four semi-empirical models (Link Cloudiness Factor (LCF), Perrin-Brichambaut (PB), Ghouard (GD), Bird Hulstrom (BH)) have been considered to predict solar radiation. An influence analysis of the seasonal variation on the quality of solar energy potential was carried out. In this study, two seasons (dry seasons and rainy season) were identified for the site of Nouakchott. Results of the study showed three cases: The first one is the clear sky, which includes two cases one was during the rainy season, where the model of the LCF was the best with Normalized Mean Square Error NMSE (0.073) and Correlation Coefficient R (0.975), and the other was during the dry season, where the model of BH was most suitable with NMSE (0.069) and R (0.973). The second case is the moderately covered sky, where the GD model was the best model during the dry season whereas BH showed the best results with NMSE (0.242) and R (0.911) during the rainy season. The third case is the covered sky, where GD model with NMSE (0.880) and R (0.831) in the dry season and PB model with NMSE (0.615) and R (0.831) in the rainy season were the most adapted ones.

Keywords: Solar energy, state of sky, prediction, solar radiation, clearness index.

INTRODUCTION

Energy is essential for human development. Fossil fuels are still widely used around the world as a principle source of energy. There are many major constraints for the environmental conservation, with an emission of about 60% of greenhouse gases (UN, 2018). Renewable energy subsector has been quite dynamic in Mauritania over the last years. Such dynamic is remarkable in 2012, through the development of a "National Strategy for the Development of the Renewable Energy Sector", and in 2014 through the integration into the initiative " Sustainable Energy for All" (SE4ALL, 2015) and also through the aiming at the increase of the proportional

*Corresponding author. E-mail: eslemhoum@gmail.com.

Author(s) agree that this article remain permanently open access under the terms of the Creative Commons Attribution License 4.0 International License

part of the renewable sources in the national energy policy to 20% by 2020 (Mario, 2015; UN, 2018). The Mauritanian country has increased the power generation capacity between 2013 and 2017. So two photovoltaic plants one of 15 MW and other of 50 MW, a wind farm of 30 MW, and hydropower from Manantali-OMVS (PNUD, 2015) were installed. The construction of a 100 MW wind farm at Boulenouar (north-west of the country) and many other small projects, operational or planned, in different localities of the country, by different operators (SOMELEC, SNIM, APAUS, ADER, etc.) reinforce the total installed capacity ((PNUD, 2015; SE4ALL, 2015). The current socio-economic context in Mauritania is very interesting in using of renewable energies, in particular the available solar source for the electricity production. However, few solar data measured are available. These are usually preliminary, short-term, and exclusive measures to prepare for the installation of new facilities. The Mauritanian solar potential has been the subject of few studies (Bilal , 2007). As a result, the solar potential is often poorly estimated, which constitutes a major constraint related to the quality of the models used for the energy estimation.

According to the geographical position, Mauritania has important solar resources. At its capital Nouakchott, located on the coast of the Atlantic Ocean, it has a significant solar potential that reaches 4.9 kWh / m2/day during the worst month (Bilal, 2007). For solar radiation modeling, conventional techniques derived from three main methods, the satellite data method, stochastic algorithms methods and empirical relationships methods are often used (Mohandes and Rehman, 2013; Cecily and al., 2013; Kostic and al., 2017; Doojdao and al., 2018). Other technics, such as artificial intelligence, are increasingly used to estimate solar radiation, namely artificial neural networks (ANNs), genetic algorithms (GAs), fuzzy logic (FL), the system adaptive neuro-fuzzy inference (ANFIS), the support vector machine (SVM) (Victor and al., 2017; Amit al., 2015; Maamar and al., 2018).

Dlamini and al. (2017) used the correlation to develop two mathematical models to estimate the global solar radiation in Swaziland, the first uses the measured monthly mean temperature and the second was based on the square root of the difference between the average of the maximum temperature and the minimum one. The results showed that there was a linear relationship between temperature and sunshine in Swaziland (Dlamini and al., 2017).

Mesri and al. (2012) developed four semi-empirical models namely Lacis and Hasen, Bird Hulstrom, Atwar and Ball and Davies and Hay for two sites in Algeria. Results showed that the Davies and Hay and Bird Hulstrom models illustrated the best estimates with the ERM (%) average error of 8.454 and 9.27 respectively for the Ghardaia site and 21.29 and 22.624 for the Bouzaréah site (Mesri and al., 2012). Dankassoua and al. (2017) used a CMP3 pyranometer to measure total solar radiation during the May-October 2013 period in Niamey (Niger), to evaluate the solar radiation potential. They used the solar radiation estimation model from the Renewable Energy Research Center (CRAER of Niger), which takes into account the humidity, aerosols and dust contained in the air (Dankassoua and al., 2017).

Makade and al. (2019) developed a single empirical model to predict monthly average daily total solar radiation (MADGSR) for different locations in India with a minimum number of input parameters, three models have been developed and compared with the literature and the real data, The study showed that the model which takes four-variable Regression Model (Sunshine Duration, latitude, altitude and Relative Humidity) indicated the best results with a mean maximum percentage error MPE of 11.89% (Makade and al., 2019)

Mohandes and Rahman (2013) compared two algorithms: optimum particle swarms (PSO) and support vector machine (SVM) to estimate the duration of sunshine in several regions in Saudi Arabia. It was concluded that the PSO model outperformed SVM.

Bosch and al. (2008) calculated the total daily solar radiation on a horizontal flat ground using an ANN model for 12 stations in Spain.

They tested different combinations of input data (daylight, extraterrestrial irradiation, clearness index, longitude, altitude, inclination, and azimuth). The optimal configuration was having as inputs the clearness index, the number of the day and 14 neurons hidden layer (Bosch and al., 2008).

Shuvho and al. (2019), used data from NASA station to predict the solar irradiation at Dhaka in Bangladesh using ANN and fuzzy logic. This study found that the performance of ANN model (with accuracy 98.78%) was better than the fuzzy logic model (with accuracy 97.47%) for solar radiation prediction.

In general, when evaluating solar radiation from semi-empirical models, several researchers use clear-sky days based on the clearness index more than 0.65. Much of the sky-based prediction methods use the clearness index without taking into account the impact of seasonal variation on the quality of the available solar potential.

This work aims to propose an approach for solar radiation prediction taking into account, at the same time, the influence of the state of the clear skies, moderately covered sky, overcast sky) and the influence of the seasons variation on the quality of the solar potential.

Concerning the solar radiation modeling, four semi-empirical models (Link Cloudiness Factor (LCF), Perrin-Brichambaut (PB), Ghouard (GD), Bird Hulstrom (BH)) are used in this study to predict solar radiation. A performance analysis of these models is performed through five indicators (Normalised Mean Square Error (NMSE), Normalized Mean Absolute Error (NMAE), Sigma

Figure 1. Geographical location of Cheikh Zayed Central Nouakchott.

Normalized mean absolute error (SNMAE), Root Mean Square Error (RMSE), Fitting Rate (R). The paper organizes as it follows: Section 2 recalls the description of the site and data collected. Next, Section 3 presents the solar radiation prediction models. .. Analysis of the state sky and the seasonal variation influence approach are presented in Section 4 fallowed by results and discussion in section 5,. Lastly, section 6 summarizes the works introduced in this paper

MATERIALS AND METHODS

The site of study is located in the northwestern of Nouakchott, the capital of Mauritania. it is positioned at 18.153 latitude, -15.983 longitude and 4 m above sea level. 15 MW solar power plant Cheikh Zayed was installed in 2013 by the Masdar Institute of Science and Technology of the United Arab Emirate. The plant is instrumented by a measurement system, every 5 min, meteorological parameters namely, solar radiation, wind speed at the surface of the panels, temperature and energy parameters (current, voltage, frequency, etc). The data collected cover the period of a year (from 01/01/ to 31/12/2016). They were used to estimate the seasonal solar radiation potential on flat ground and to validate solar radiation models prediction for different state of sky. Figure 1 shows the geographical location of the site.

Solar radiation prediction models

This section presents the approach used to predict the solar radiation, taking into account the state of the sky and the periods of season. The studied models are Ghouard, Perrin-Brichambaut, Bird Hulstom and Linkcloud factor. Table 1 presents the semi-empirical models used to estimate the total solar radiation (Dankassoua and al., 2017 ; Bosch and al., 2008 ; Perrin-Brichambaut, 1975 ; Bird Hulstrom, 1981 ; Saighi and al., 2002 ; Mghouchi and al., 2016 ; Yettou and al., 2009). Table 2 presents the parameters of solar geometry useful for the calculation of solar radiation and available energy (Mesri and al., 2012 ; Dankassoua and al., 2017 ; Kerkouche and al., 2013 ; Daguenet, 1985). Table 3 illustrates the statistical indicators used to evaluate the performance of each model (Bilal and al., 2018 ; Kerkouche and al., 2013).

Approach to analyze the influence the sky state and seasonal variation on the solar potential

The solar radiation data collected at the Nouakchott site are used to characterize and model the available solar radiation according to the following steps:

(i) Extra-terrestrial solar energy is calculated first.
(ii) Determination of the clearness index for each day of the year.
(iii) Classify the data on the period of one year to two seasons based on available solar energy
(iv) Classify the days of each season in three parts according to the sky condition: clear sky, moderately covered sky, and covered sky.
(v) Model and characterize solar radiation by season for different stat of sky.
(vi) Identification of the appropriate model for each season and each state of sky (Figure 2).

RESULTS AND DISCUSSION

Solar radiation measured on flat ground, at Nouakchott site are used to characterize the solar potential . An analysis of the measured data revealed that the coverage rate measured is 98%.The results of the available potential characterization have shown many fluctuating of the measured solar radiation which lies, between 2000 Wh/m2/d and the 8400 Wh/m2/d, due to various atmosphere absorptions. The absorption rate of solar radiation through the atmospheric layer is measured by the clearness index (ratio of solar energy measured at the ground and the extra-terrestrial solar energy). The evolution of these two types of energies is shown in Figure 3. The calculated clearness index was used to

Table 1. Different model for solar radiation prediction.

References	Models	Equations	Description of parameters
Saighi (2002)	Ghouard (GD)	$I = Ics \times e^{\frac{A1}{\sin(hs)}} \times \sin(hs)$ $D = Ics \times Ct \times \left[0.271 - 0.2939 \times A1 \times e^{\frac{-A2}{\sin(hs)} \times \sin(hs)} \right]$ $Ct = 1 + 0.034 \times \cos(n - 2)$ $G = I + D$	I : direct solar radiation (W/m²) Ics : solar constant (W/m²) A_1 et A_2: constant, depending on the nature of the ground. hs : solar height (radian). D : diffuse radiation (W/m²) Ct : correction factor due to the variation of the distance earth-sun n : number of the day grille (-) G : global radiation (W/m²)
Perrin Brichambaut, (1975); Mghouchi and al. (2016)	Perrin-Brichambaut (PB)	$I = R \times e^{\left(\frac{-A}{B \times \sin(hs+1)}\right) \times \sin(hs)}$ $D = 0.1 \times Ics \times Ct \times (\sin(hs))^{0.4}$ $G = I + D$	I : direct solar radiation(W/m²) A, B, et R : constants according to sky condition hs : solar height (radian). D : diffuse radiation (W/m²) Ics : solar constant (W/m²) Ct : correction factor due to the variation of the distance earth sun G : total radiation (W/m²)
Dankassoua et al. (2013); Bilal and al. (2017) ; Yettou et al. (2009)	Link Cloudiness Factor (FTL)	$I = Ics \times e^{\frac{(-1L)}{(0.9+9.4 \times \sin(hs)) \times \sin(hs)}}$ $D = 0.04 \times Ics \times \sqrt{\sin(hs)} \times \left(TL - 0.5 - \sqrt{\sin(hs)}\right)$ $TL = 2.4 + 14.6 \times Fta + 0.4 \times (1 + 2Fta) \times \ln(Pr)$ $G = I \times \sin(hs) + D$	I : direct solar radiation(W/m²) Ics : solar constant (W/m²) TL : Link trouble factor (-) hs : solar height (radian). D : diffuse radiation (W / m²) Fta: atmospheric disturbance factor. Pr : partial pressure of water vapor (mmHg) G : Total solar radiation (W/m²)
Perrin-Brichambaut, (1975) ; Mghouchi and al. (2016)	Bird Hulstrom (BH)	$I = 0.9751 \times Ics \times Tr \times To \times Tg \times Tw \times Ta$ $D = Dr + Da + Dm$ $G = I \times \sin(hs) + D$	I : direct solar radiation(W/m²) Ics : solar constant (W/m²) Tr, To, Tg, Tw et Ta : Rayleigh transmission factors (-) Dr : Rayleigh scattering (W/m²) Da : aerosol dispersion (W/m²) Dm : process of multi-reflection between the sky and the ground (W/m²). D : diffuse radiation (W/m²) G : Total radiation (W/m²)

classify the days of the year according to the state of sky (clear sky, covered sky, and moderately covered sky).

Table 2. Solar geometry models.

References	Models	Equations	Description of parameters
Kerkouche and al. (2013); Daguenet, (1985)	Solar declination	$\theta = 23.45 \times \sin\left(360 \times \frac{(284+n)}{365}\right)$	θ: solar declination (°) n : number of the day in the year (from 1 to 366)
Dankassoua and al. (2017) ; Kerkouche and al. (2013); Daguenet, (1985)	Hour angle	$\omega = 15 \times (\text{tsv} - 12)$	ω : hour angle (°) tsv : true solar time (h)
Daguenet (1985)	Solar height	$\sin(\text{hs}) = \sin(\varphi) \times \sin(\theta) + \cos(\varphi) \times \cos(\theta) \times \cos(\omega)$	hs: solar height (°) φ : latitude of place (°) θ: solar declination (°) ω : hour angle (°)
Kerkouche and al. (2013); Daguenet, (1985)	Daily extra-terrestrial solar energy	$\text{Go} = \frac{24 \times \text{Ics}}{\pi} \times \left[1 + 0.033 \times \cos\left(\frac{360 \times \text{n}}{365}\right)\right] \times \left[\cos(\theta) \times \cos(\varphi) \times \sin(Ws) + \frac{\pi}{180} \times Ws \times \sin(\varphi) \times \sin(\theta)\right]$ $\text{Ws} = \cos\text{-}1 \times [-\tan(\varphi) \times \tan(\delta)]$	Go : extra-terrestrial solar energy (Wh/m²) Ics : solar constant (W/m²) n : number of day in the year (from 1 to 366) θ: solar declination (°) φ : latitude of place (°) Ws :hour angle sunrise (°)
Daguenet (1985)	Measured energy	$\text{Gm} = \int_{\text{Ls}}^{\text{Cs}} \text{I(t)} \times dt$	Gm : Daily solar energy measured at the ground (Wh/m²) Ls : sunrise time (h) Cs : sunset time (h) I(t) : measured instantaneous radiation (W/m²)
(Mesri and al., (2012); Dankassoua and al. (2017) ; Kerkouche and al. (2013)	Clearness index	$\text{k} = \frac{\text{Gm}}{\text{Go}}$	Kt : clearness index (-) Gm : Daily solar energy measured on the ground (Wh/m²) Go : extra-terrestrial solar energy e (Wh/m²)

The results on the clearness index (k) calculation are used to classify the year to three type of days, according to the covered sky condition: a). the days where the clearness index is less than 0.35, b) the days where the clearness index lies between 0.35 and 0.65 and c) the days where the clearness index is higher than 0.65. The first type of days corresponds to the covered sky, the second one corresponds to the days with moderately covered sky and the third type of days shows a clear sky. The distribution of the clearness index for each period type of days is illustrated in the Figure 4. It appeared that the covered days, characterized by clearness index k≤0.35, have a maximum percentage of 1.5% and

Table 3. Statistical indicators of the performance models.

References	Models	Equations	Description of parameters
Bilal and al. (2018)	Normalized Mean Square Error (NMSE)	$\mathrm{NMSE} = \frac{\sum_{i=1}^{n}(\mathrm{Yo} - \mathrm{Ym})^2}{\sum_{i=1}^{n}(\mathrm{Yo} - \mathrm{Ya})^2}$ $Ya = \frac{\sum_{i=1}^{n} Ym}{k}$	Yo : predicted values (W/m²) Ym : measured values (W/m²) K : number of data (-)
Bilal and al. (2018)	*Normalized Mean Absolute Error*(NMAE)	$\mathrm{NMAE} = \frac{\sum_{i=1}^{n}\lvert Yo - Ym\rvert}{\sum_{i=1}^{n}\lvert Yo - Ya\rvert}$	Yo : predicted values (W/m²) Ym : measured values (W/m²)
Bilal and al. (2018)	Sigma Normalized mean absolute error (SNMAE)	$\mathrm{SNMAE} = \frac{\sum_{i=1}^{n}\lvert Yo - Ym\rvert}{\sqrt{\sum_{i=1}^{n}(\mathrm{Yo} - \mathrm{Ya})^2}}$	Yo : predicted values (W/m²) Ym : measured values (W/m²)
Kerkouche and al. (2013)	Root Mean Square Error (RMSE)	$RMSE = \sqrt{\frac{\sum_{i=1}^{n}(Yo - Ym)^2}{k}}$	Yo : predicted values (W/m²) Ym : measured values (W/m²) K : number of data (-)
Bilal and al. (2018)	Correlation Coefficient (R)	$R = \frac{\mathrm{cov}(Yo, Ym)}{\sqrt{\mathrm{var}(Yo)} \times \sqrt{\mathrm{var}(Ym)}}$	Yo : predicted values Ym : measured values

an almost zero distribution that means the total cloudy covered sky is rare. For moderately covered sky, where clearness index 0.35> k≥0.65, there is a large distribution that converges the upper limit (k = 0.65) of the interval with a maximum percentage of about 14.1%. For the clear sky, where k> 0.65, the interval contains the largest distribution of the clearness index, were the values ranges from 0.65 to 0.9 with the highest frequency of 12%, observed for clearness index of 0.73.

Further, it could be noted that a significant number of days "moderately covered" is about 30% of the days in the year, where the highest energy reaches 7173 Wh/m2/d (case of the day number 180,in the dry season, clearness index of 0.644). In addition, during the rainy season, for the same state of sky (moderately covered sky), the measured energy reaches 7168.7 Wh/m2 /d (case of the day number 194 with clearness index 0.645). This result shows that for a moderately covered sky, a higher clearness index does not necessarily correspond to a higher energy. Figure 5 shows the variation of the solar radiation for a typical day of each state of sky, according to the dry season and to the rainy season.

During the rainy season (June to October), we observed that: the Daytime radiation, for the moderately covered sky are highly disturbed due to the precipitation and cloudiness of the season (Figure 5a). On the other hand, the radiations of days in clear sky, show a regular variation without disturbance, because of the low attenuation of the atmospheric layers, making these days among the sunniest of the year (1080 W/m2/d). The frequencies (Figure 5.b) in the covered sky condition are 90% for solar radiation between 0 and 500 W/m2/d. It is only 10% for radiation between 500 and 600 W/m2/d. For the moderately

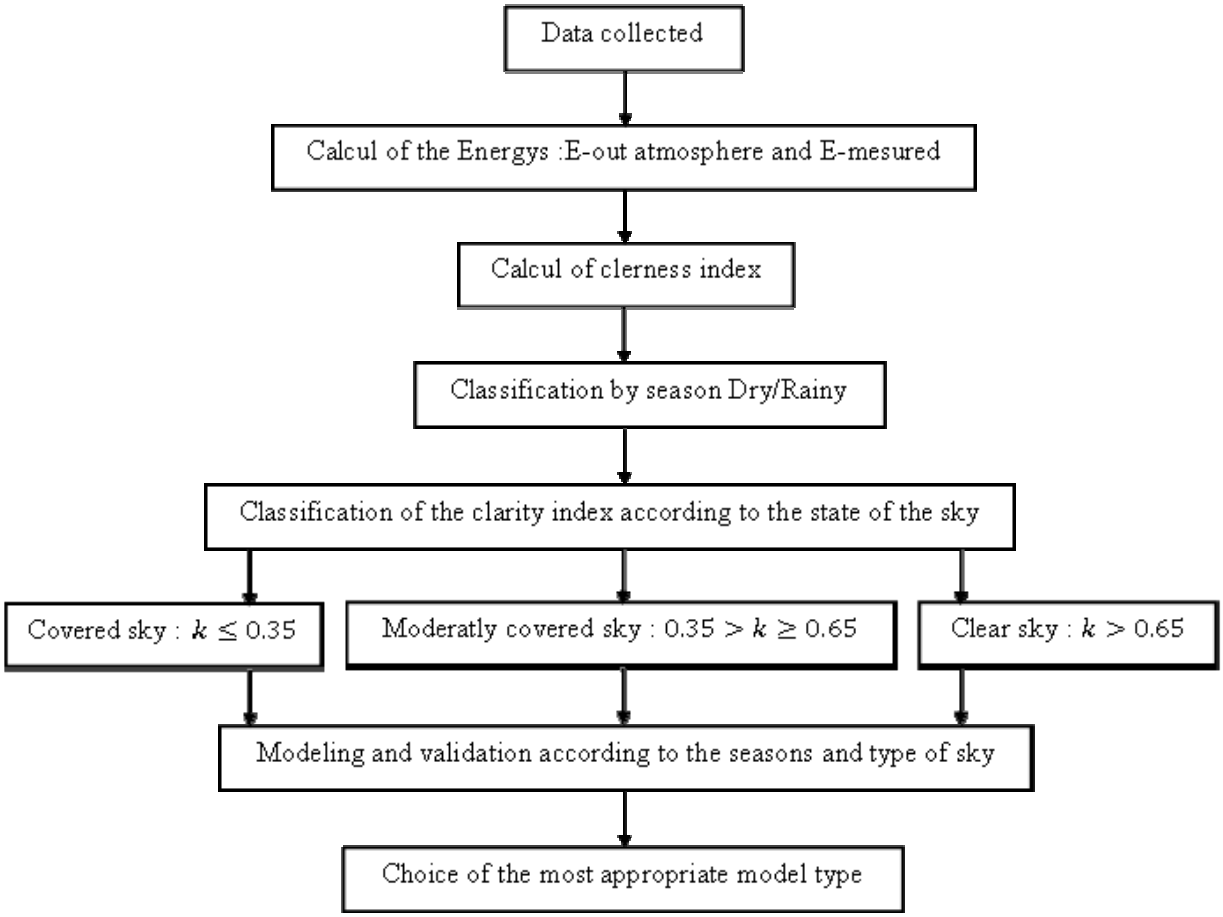

Figure 2. Data processing architecture algorithm.

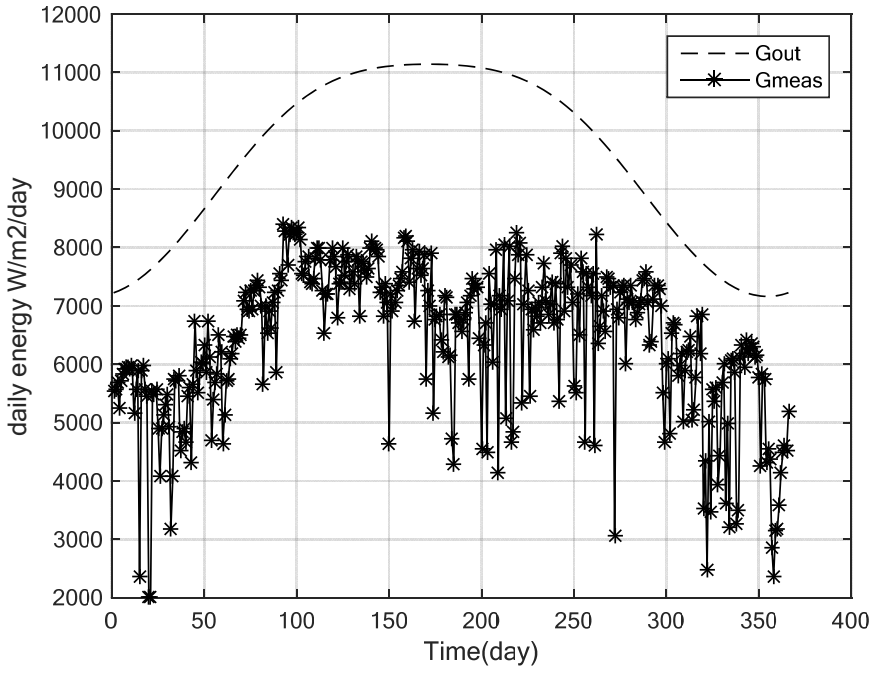

Figure 3. Daily extraterrestrial solar energy and the measured at the ground.

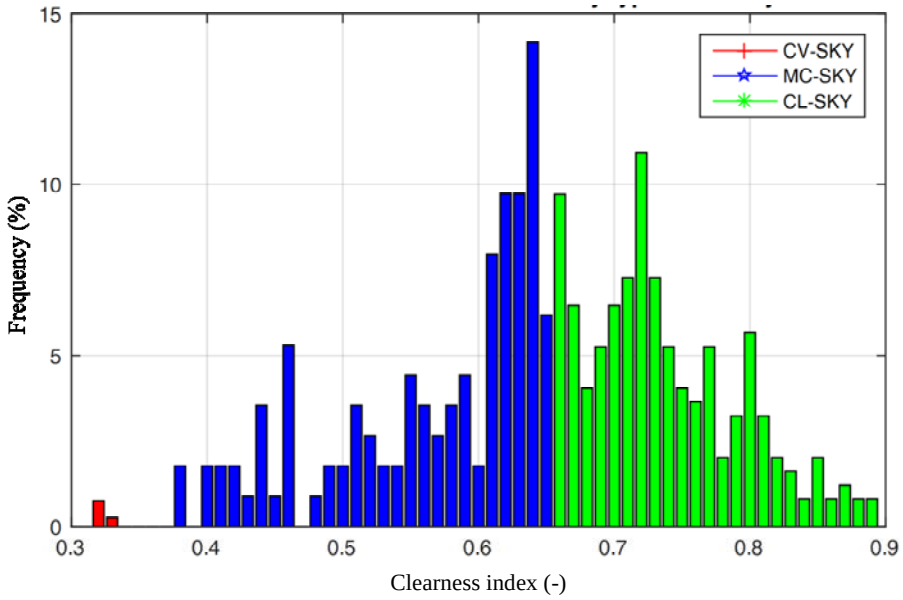

Figure 4. Frequency distribution of the clarity index.

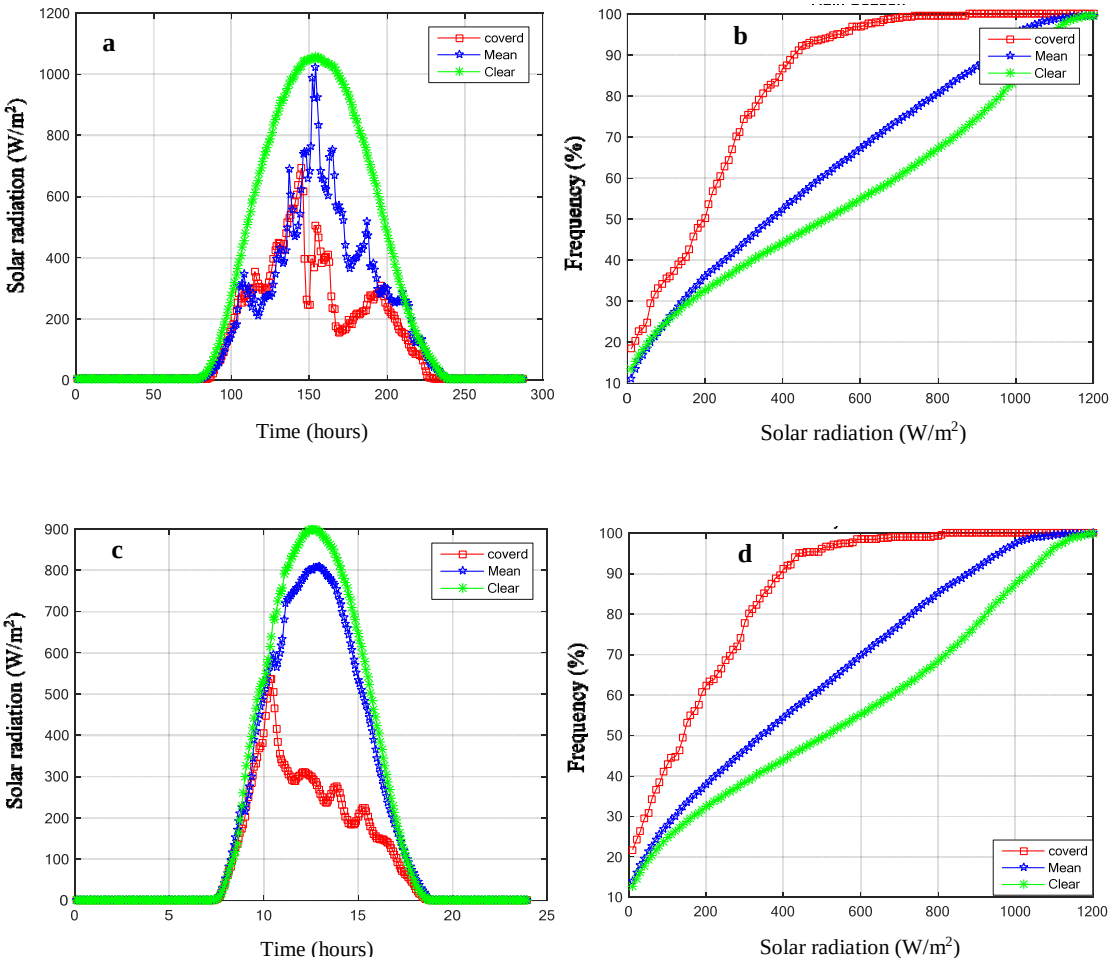

Figure 5. Evolution of daily solar radiation and of cumulative frequency distribution according to the state of the sky: (a) and (b) rainy season, (c) and (d) dry season: period of one year.

sky condition, the frequencies are 60% for for the solar radiation between 0 and 600 W/m2/d and 40% for solar radiation between 600 and 1100 W/m2/d. While for the clear sky condition, the cumulative frequency is 50% for solar radiation between 600 and 1160 W/m2/d. For the dry season (November to October), as shown in Figure 5c and d) it can be noted that the solar radiation attenuation for the case of the covered sky are negligible. The clearness index corresponding to this type of day are around 0.35 (upper limit of this type of sky), as shown in Figure 4. In the case of days with moderately covered sky, the solar radiation is visibly attenuated (the measured solar radiation peak is 600 W/m2/d). The distribution of the solar radiation for the case of moderately covered the sky moderately covered is represented by a curve almost aligned. It can be noted that 40% of these frequencies are between 600-1000 W/m2/d. Also for the days with clear sky, 50% of the frequencies are between 600 and 1200 W/m2/d, which explains why a photovoltaic generator installed in this zone can operate at 50% of its time giving a power between 600-1200 W/m2/d.

Modeling of solar radiation

The solar radiation modeling for the two seasons was carried out considering the astronomical data (geographical coordinates, solar height ...) and the attenuation factors according to the state of sky. Four models (Ghouard, Perrin-Brichambaut, Bird Hulstom and Link Cloudiness Factor) were studied. The results of this study are illustrated by the Figure 6. They are given as the variation of solar radiation towards the time. For the both seasons and for each state of sky. Results show that the sunrise and the sunset correspond for the real data and for the models. However, the time of the maximum of the solar radiation corresponds for the cases of Figure 6c, 6d, 6e and 6f. For the Figure 6a and 6b, the measured solar radiation has attenuations that the time of the peak of the solar radiation is different from that of the model.

The solar radiation measured and estimated for every five minutes are used to analyze the quality of the available solar potential. The cumulative distribution of the solar radiation is then determined for each season and for each state of sky. Figure 7 shows the cumulative frequency distribution according to the state of the sky and by season. It can be noted that, for a clear sky (Figure 7a and b), the Bird Hulstrom and Link Cloudiness Factor models are the closest with 90% of the cumulative frequencies which has solar radiation lower then 1000 W/m2/d during the dry season and during the rainy season. Figure 7c and d illustrate the case of the moderately overcast sky during the dry and the rainy season respectively. The Ghouard and Bird Hulstrom models are closer to the measure with 80% of cumulative frequencies having a solar radiation less than 800 W/m2/d during the dry season, and 80% of cumulative frequency for the solar radiation less than 770 W/m2/d during the rainy season.

In the case of covered sky (Figure 7e and f), it can be observed that during the dry season, the closest models to the measures are Ghouard with 70% of frequencies for the radiation less than or equal to 420 W/m2/d. During the rainy season and model of Perrin-Brichambaut is the most powerful, where 90% of frequencies corresponds to a solar radiation less than 420 W/m2/d.

Model performance analysis

The performance of the models was studied for the two seasons (dry season and rainy season) and for the three cases of the sky types (clear sky, moderately covered sky and covered sky).The choice of the most appropriate model was made based on the performance indicators named: the Normalized Mean Square Error (NMSE), Normalized Mean Absolute Error (NMAE), Segma Normalized Mean Absolute Error (SNMAE), Root Mean Square Error (RMSE) and the Fitting Rate (R). Results on the calculation of these indicators are shown in Table 4.

Table 4 illustrates that, for a clear sky, Link Cloudiness Factor model shows better performance during the rainy season with NMSE (0.073) and R (0.975) while for the dry season it is the model of Bird Hulstrom which gives the best performance with NMSE (0.069) and R (0.973). In the case of moderately overcast sky, the Ghouard model estimates better the solar radiation during the dry season, with NMSE (0.186) and R (0.933), while during the rainy season it is Bird Hulstrom's with NMSE (0.242) and R (0.911). In the case of a covered sky, the most indicated models are, Ghouard for the dry season with NMSE (0.880) and R (0.831), and Perrin-Brichambaut for the rainy season with NMSE (0.615) and R (0.831).

Figure 8 illustrates the distribution of the daily energy according to the state of sky and the season for the site of Nouakchott. Figures 8a and b, respectively, show the corresponding distribution for the dry season and for the rainy season, Figure 8c and d illustrate the distribution of energies for the case of moderately overcast sky for the dry season and for the rainy season, respectively. For the case of clear sky is shown in Figure 8e for the dry season and Figure 8f for the rainy season. These various results have allowed to made the following observations.

(i) For the overcast sky, during both the dry and the rainy seasons, all models overestimate the extent, however the Ghouard model presents the best estimation.

(ii) For moderately covered sky, during the dry season, the measurements are between 2826-7051 Wh/m2/d. However, Ghouard model provides a better estimate of solar radiation during the rainy season (Figure 8d). The measures solar radiation varies between 3222-7168 Wh/m2/d.

(iii) For the clear sky, during the both dry and rainy

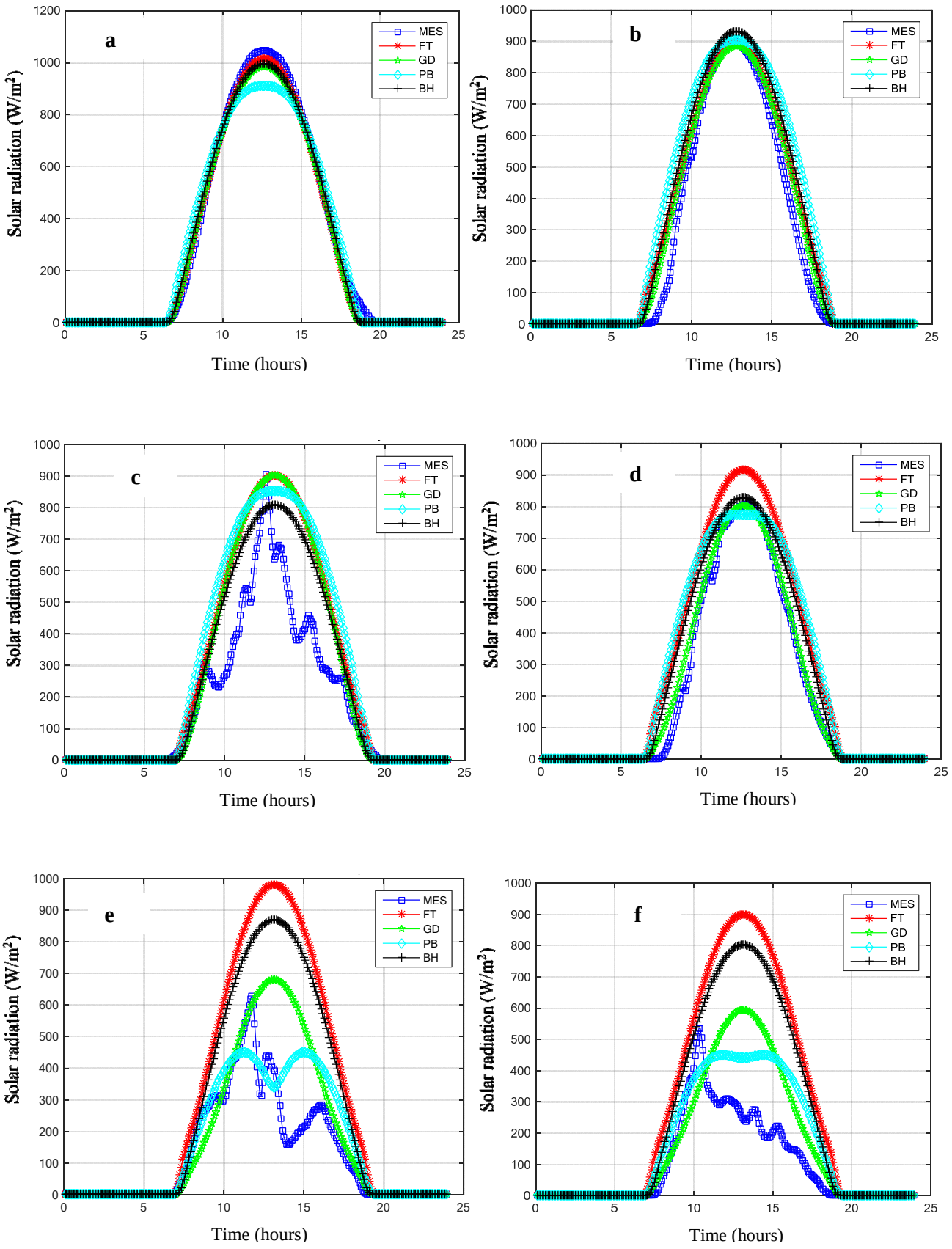

Figure 6. Estimation of daily average solar radiation: (a) and (b) clear sky for the rainy and the dry season, (c) and (d) moderately covered sky for the rainy and the dry season, (e) and (f) covered sky for the rainy and dry season respectively.

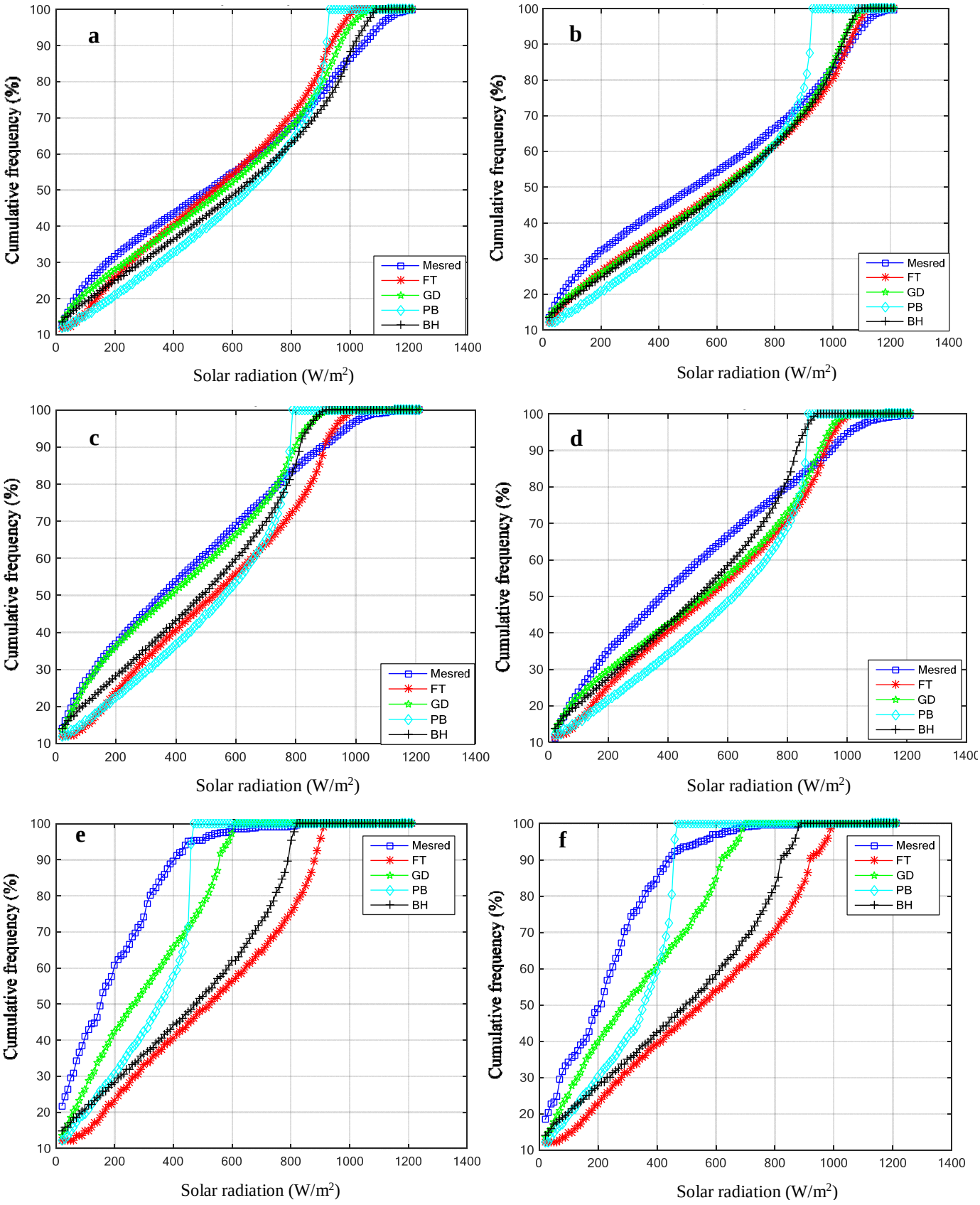

Figure 7. Cumulative frequency distribution of solar irradiation: (a) and (b) clear sky for the dry and the rainy season, (c) and (d) moderately covered sky for the dry and the rainy season, (e) and (f) covered sky for the dry and the rainy season respectively.

Table 4. Indicators performance of the models for every season and for every state of sky.

State of Sky	Models	NMSE		NMAE		SNMAE		RMSE		R	
		DS	RS	DS	RS	DS	RS	DS	RS	DS	RS
Clear sky	Link Cloudiness Factor (LCF).	0.072	0.073	0.226	0.202	32.279	22.640	104.394	107.787	0.972	0.975
	Ghouard(GD)	0.078	0.077	0.227	0.212	32.327	23.695	109.051	110.579	0.971	0.971
	Perrin-Brichambaut (PB)	0.128	0.134	0.313	0.318	44.551	35.584	139.321	146.010	0.953	0.952
	BirdHulstrom(BH)	0.069	0.082	0.220	0.220	31.382	24.672	102.119	114.347	0.973	0.971
moderately covered sky	Link Cloudiness Factor (LCF).	0.297	0.294	0.460	0.441	39.106	36.402	177.611	185.588	0.917	0.904
	Ghouard (GD)	0.186	0.268	0.365	0.415	31.013	34.238	140.538	177.317	0.933	0.908
	Perrin-Brichambaut (PB)	0.307	0.354	0.485	0.510	41.176	42.111	180.801	203.640	0.900	0.896
	BirdHulstrom(BH)	0.220	0.242	0.395	0.414	33.548	34.216	153.152	168.278	0.918	0.911
covered sky	Link Cloudiness Factor (LCF).	5.0413	4.685	2.2962	2.178	34.092	31.991	368.869	376.004	0.827	0.820
	Ghouard (GD)	0.880	0.997	0.8811	0.851	13.082	12.50	154.144	173.486	0.831	0.824
	Perrin-Brichambaut (PB)	0.892	0.615	0.9475	0.761	14.067	11.17	155.202	136.312	0.816	0.831
	BirdHulstrom(BH)	3.555	3.251	1.8723	1.749	27.798	25.68	309.772	313.221	0.823	0.818

seasons (Figure 8e and f respectively), the predictions of the different models are quite close and are around the measures

Conclusion

The objective of this paper was to model the solar radiation for different state of the sky and for the seasonal variation. The study allowed to implement an approach to characterize solar radiation and identify the most appropriate model to estimate the solar radiation .The data measured for every 5-minute during 2016 on the site of Cheikh Zayed power station in Nouakchott, were used in this study.

The calculation of the clearness index made it possible to define three types of sky according to seasons. The distribution of daily clearness index by type of sky showed for 2016, that the number of days corresponding to clear sky was the most important (68.5%), followed by the days with medium coverage sky (30%). It can be seen that for a moderately overcast sky, a higher clearness index did not necessarily correspond to higher energy.

Then four semi empirical models, taking into account, at the same time, the state of the sky and the season, are studied. Results were analyzed through five statistical performance indicators. It was noted that for a moderately covered sky, the models of Ghouard and Bird-Hulstrom estimate better the solar radiation during the dry and the rainy season respectively. While for the clear sky the Bird & Hulstrom models and Link Cloudiness Factor were the best for both the dry and the rainy season respectively. Regarding to covered sky, the models of Ghouard and Perrin- Brichambaut were the best.

The distribution of daily energy in Nouakchott according to the state of the sky and the season has shown that:

- For the overcast sky, all models overestimated energy. Whatever the season, the best evaluation is observed for the model Ghouard.
- For the moderately overcast, during the dry season, energy highly dispersion.
-For the clear sky, the predictions of the various models are quite close and are around the real values during the two seasons, with overall a tendency to overestimate.

The use of current models allows prediction of the solar radiation, in order to evaluate, subsequently, the solar potential. A better prediction contributes to better size devices of solar system for electrical conversion and optimization. So, it is very interesting.

To analyze the potential solar energy considering

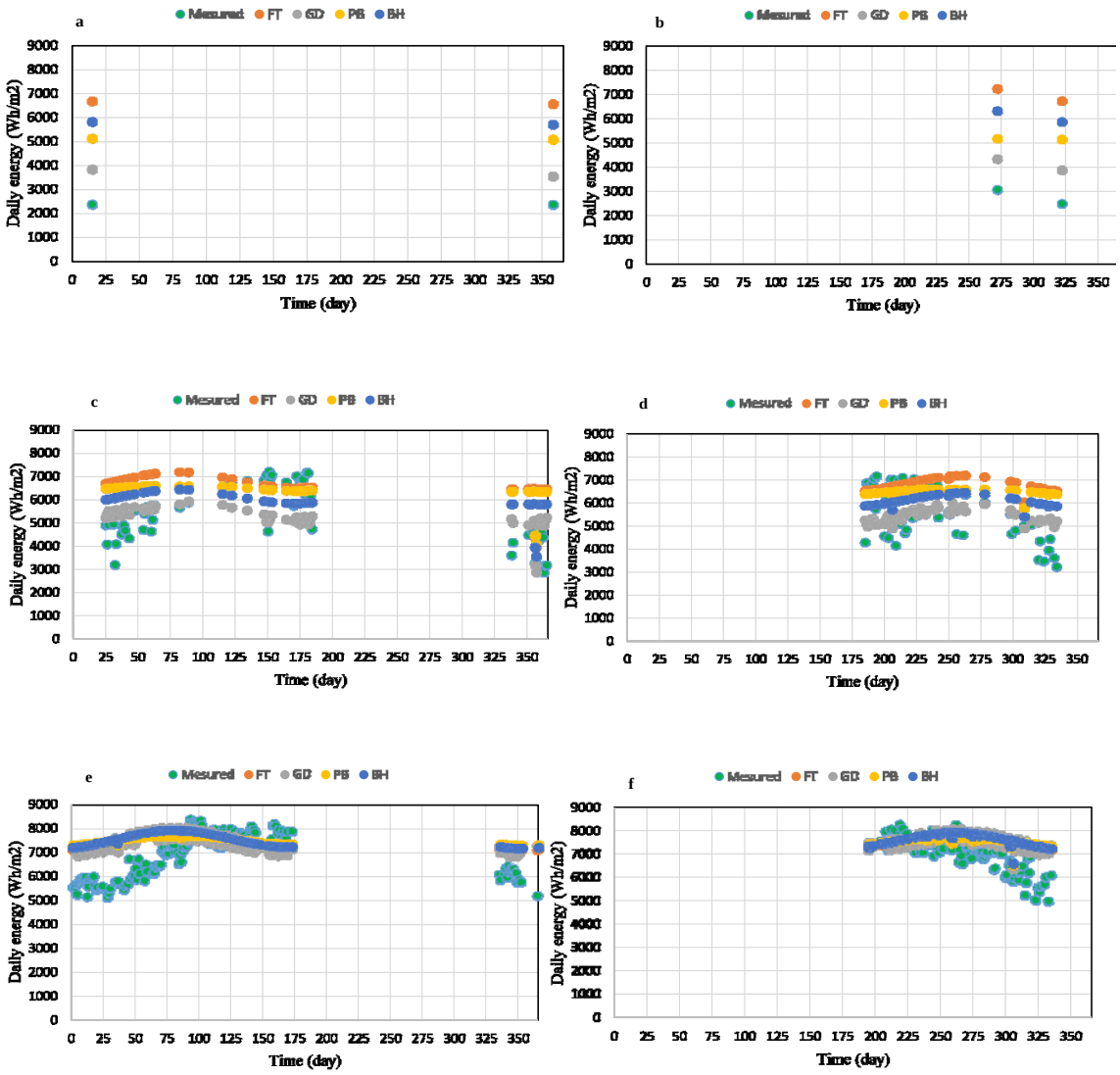

Figure 8. Daily energy distribution according to the state of the sky and the season (Nouakchott, 2016): covered sky for the dry season (a), covered sky for the rainy season (b), moderately covered sky for dry season (c) sky moderately covered sky for the rainy season (d), clear sky for the dry season (e) clear sky for the rainy season (f).

the spectral distribution of solar radiation according to the atmospheric composition or Sahelian region.

NOMANCLATURE

A: constants according to sky condition (-)
Cs: sunset time(h)
Ct:: correction factor due to the variation of the distance earth sun(min)
D: diffuse solar radiation (W/m2)
Dr: Rayleigh scattering (W/m2)
Da: aerosol dispersion (W/m2)
Dm: process of multi-reflection between the sky and the ground (W/m2).
Fta: atmospheric disturbance factor (-).
Gm: Daily solar energy measured on the ground (Wh/m²)
Go:Daily solar energy out the atmosphere (Wh/m²)
G: global radiation (W/m2)
hs: solar height (°).
I:direct solar radiation (W/m2)
Ics: solarconstante (W/m2)
I(t) :): measured instantaneous solar radiation
K: number of data
Kt: clearness index (-)
Ls: sunrise time (h)
n: number of the day in the year (from 1 to 366)
Pr: partial pressure of water vapor (mmHg)
R: constants according to sky condition (-)
TL: trouble factor fo Link (-)

Tr,To,Tg,Tw et Ta : Rayleigh transmission factors (-)
tsv: true solar time (h)
Ws: hour angle sunrise (°)
Yo: predicted values (W/m²)
Ym: measured values (W/m²)
θ: solar declination (°)
ω: hour angle (°)
φ: latitude of place (°)
DS: dry season
RS: rainy season

CONFLICT OF INTERESTS

The authors have not declared any conflict of interests.

REFERENCES

Amit KY, Hasmat M, Chandel SS (2015). Application of rapid miner in ANN based prediction of solar radiation for assessment of solar energy resource potential of 76 sites in Northwestern India. Renewable and Sustainable Energy Reviews 52:1093-1106.

Bilal B, Ndongo M, Kebe CMF, Ndiaye PA, Sambou V (2018). Wind Turbine Power Output Prediction Model Design Based on Artificial Neural Networks and Climatic Spatiotemporal Data. IEEE 1085-1092.

Bilal B, Sambou V, Kebe CMF, Ndiaye PA, Ndongo M (2007). Etude et modélisation du potentiel solair du site Nouakchott et de Dakar, Journal des sciences 7:57-66.

Bird RE, Hulstrom RL (1981). Simplified clear sky model for direct and diffuse insolation on horizontal surfaces (No. SERI/TR-642-761). Solar Energy Research Inst., Golden, CO (USA).

Bosch JL, Lopez G, Batlles FJ (2008). Daily Solar Irradiation Estimation over a Mountainous Area using Artificial Neural Networks. Renewable Energy 33:1622-1628.

Cecily N, Raymond K, Urias G (2013). Modelling of solar radiation for West Africa: The Nigerian option. International Journal of Physical Sciences 8(28):1458-1463.

Daguenet M (1985). Les sechoirs solaires : théorie et pratique. https://unesdoc.unesco.org/ark:/48223/pf0000123413

Dankassoua M, Madougou S, Aboubacar A, Foulani A (2017). Etude du rayonnement solaire global à Niamey de la période de pré-mousson et de la mousson de l'année 2013 (mai à octobre). Revue des Energies Renouvelables 20:131-146.

Dlamini MD, Varkey AJ, Mkhonta SK (2017). Models for calculatingmonthlyaveragesolar radiation from air temperature in Swaziland. International Journal of Physical Sciences 2:247-254.

Doojdao C, Choosri P, Janjai S, Buntoung S, Nunez M, Thongrasmee W (2018). A semi-empirical model for estimating diffuse solar near infrared radiation in Thailand using ground- and satellite-based data for mapping applications. Renewable Energy 117:175-183

Kerkouche K, Cherfa F, Hadj A, Bouchakour S, Abdeladim K, Bergheul K (2013). Evaluation de l'irradiation solaire globale sur une surface inclinée selon différents modèles pour le site de Bouzaréah. Revue des Energies Renouvelables 16:269-284.

Kostic R, Mikulovic J (2017). The empirical models for estimating solar insolation in Serbia by using meteorological data on cloudiness. Renew Energy 114:1281-1293.

Maamar L, Salah H, Abdallah HA (2018). Novel Approach for Estimating Monthly Sunshine Duration Using Artificial Neural Networks: A Case Study. Journal of Sustainable Development of Energy, Water and Environment Systems 7:405-414.

Makade RG,Chahakrabati S,Jamil B (2019). Prediction of global solar radiation using a single empirical model for diversified locations across India. Urban Climate Elsevier 29:100492.

Mario S (2015). Représentant résident PNUD en Mauritanie « évaluation de l'état de préparation aux énergies renouvelables », International RenewableEnergy Agency (IRENA).

Mesri MM, Rougab I, Cheknane A, Bachari NI (2012). Estimation du rayonnement solaire au sol par des modèles semi-empiriques. Revue des Energies Renouvelables 15:451-463

Mghouchi Y, El bouardi A, Choulli Z, Ajzoul T (2016). Modèle for obtaining the daily direct, diffuse and global solar radiations. Renewable and Sustainable Energy Reviews 56:87-99.

Mohandes MA, Rehman S (2013). Estimation of Sunshine duration in Saudi Arabia. Journal of Renewable and Sustainable Energy 5:1-14.

Perrin-Brichambaut C (1975). Estimation des ressources énergétique en France, cahiers de L'AFEDS, N°1.

SE4ALL (2015). Mauritanie- Evaluation et Analyse des Gaps, Energie Durable pour Tous à l'horizon 2030 à l'initiative « Énergie durable pour tous, Sustainable Energy for All, SE4ALL.

Saighi M (2002). Nouveau modèle de transfert hybride dans le système solaire platform atmosphère, thèse de doctorat, Alger, USTHB.

Shuvho MBA, Chowdhury MA, Ahmed S, Abul Kashem M (2019). Prediction of solar irradiation and performance evaluation of grid connected solar 80KWp PV plant in Bangladesh. Energy Reports Elsevier 5:714-722.

UN (2018). Accroître nettement la part de l'énergie renouvelable d'ici à 2030 : le rôle de la science, de la technologie et de l'innovation, Nations Unies, Commission de la science et de la technique au service du développement Vingt et unième session Genève.

Victor HQ, Javier A, Javier AA, Laurel S (2017). ANFIS, SVM and ANN soft-computing techniques to estimate daily global solar radiation in a warm sub-humid environment. Journal of Atmospheric and Solar–Terrestrial Physics 155:62-70.

Yettou F, Malek A, Haddadi M, Gama A (2009). Etude comparative de deux modèles de calcul du rayonnement solaire par ciel clair en Algérie, Revue des Energie Renouvelable 12:331-346.